Available online at www.sciencedirect.com
ScienceDirect
Polymer 47 (2006) 7900–7908
polymer
www.elsevier.com/locate/polymer

Nitroxide-mediated radical polymerization of styrene: Experimental evidence of chain transfer to monomer

Per B. Zetterlund [a], Yuichi Saka [b], Ronan McHale [c], Tadashi Nakamura [b], Fawaz Aldabbagh [c], Masayoshi Okubo [a,b,*]

[a] *Department of Chemical Science and Engineering, Faculty of Engineering, Kobe University, Kobe 657-8501, Japan*
[b] *Graduate School of Science and Technology, Kobe University, Kobe 657-8501, Japan*
[c] *Department of Chemistry, National University of Ireland, Galway, Ireland*

Received 31 July 2006; received in revised form 15 September 2006; accepted 19 September 2006
Available online 10 October 2006

Abstract

Chain transfer to monomer during nitroxide-mediated radical polymerization of styrene has been investigated for 2,2,6,6-tetramethylpiperidinyl-1-oxy (TEMPO) and *N-tert*-butyl-*N*-(1-diethylphosphono-2,2-dimethylpropyl) nitroxide (SG1) mediated polymerizations at 125 and 110 °C, respectively. A novel technique employing a fluorescence-labelled polystyrene–TEMPO macroinitiator enabled separate detection of the total chain distribution and the distribution of chains containing the original macroinitiator, thus directly confirming the presence of chains not containing macroinitiator. Chain transfer to monomer results in a low molecular weight tail, which can be very much pronounced, in particular in the number distributions. Quantitative analysis of the total number of chains in both the TEMPO and the SG1 systems, correcting for the contribution of thermal initiation of styrene, yielded chain transfer to monomer constants in agreement with the literature.

Keywords: Controlled/living radical polymerization; Chain transfer; Nitroxide

1. Introduction

Controlled/living radical polymerization (CLRP) enables synthesis of polymers with narrow molecular weight distributions (MWDs), predetermined molecular weights and various complex architectures [1,2]. The three most well-known CLRP techniques are nitroxide-mediated polymerization (NMP) [3], atom transfer radical polymerization (ATRP) [4], and reversible addition-fragmentation chain transfer (RAFT) polymerization [5]. In order to improve current CLRP systems and to develop new more efficient systems, it is important not only to understand the chemistry of the activation–deactivation mechanism involving propagating radicals, but also any side reactions which may compromise the efficiency of the process.

A number of side reactions occur in NMP systems, the relative significance of which depends on the particular system. These include termination between propagating radicals [2], alkoxyamine decomposition to yield terminally unsaturated polymer and hydroxylamine [6–10], hydrogen transfer between a propagating radical and hydroxylamine [10,11], and nitroxide decomposition [12,13]. Strictly speaking, termination is not a side reaction because a certain level of termination is a requirement for the persistent radical effect to be operative (the fundamental reason the system is controlled/living in the first place) [14], but excessive termination is obviously not desirable. However, generally speaking, all of the above processes have adverse effects on the polymerization process. A side reaction, which has perhaps received less attention, is chain transfer to monomer. Chain transfer to monomer results in: (i) irreversible deactivation of a propagating radical, and (ii) generation of a new chain by initiation by a monomeric

* Corresponding author. Department of Chemical Science and Engineering, Faculty of Engineering, Kobe University, Kobe 657-8501, Japan. Tel./fax: +81 78 803 6443.
E-mail address: okubo@kobe-u.ac.jp (M. Okubo).

0032-3861/$ - see front matter © 2006 Published by Elsevier Ltd.
doi:10.1016/j.polymer.2006.09.033

radical (in the case of styrene (S), it has been proposed that chain transfer to monomer may in fact be to the Diels–Alder adduct formed by the reaction of two S units [15,16]), both of which are detrimental to a CLRP process. Thus, chain transfer to monomer affects both the ''livingness'' (the fraction of chains being ''dormant'' species, capable of undergoing chain extension) and the control (the narrowness of the MWD) of the polymerization.

According to simulations by Greszta and Matyjaszewski of 2,2,6,6-tetramethylpiperidinyl-1-oxy (TEMPO)-mediated radical polymerization of S at 120 °C, transfer to monomer leads to a relatively small but significant increase in polydispersity (M_w/M_n) [17]. The number of dead chains formed by chain transfer to monomer was higher than by termination, but most dead chains were formed by alkoxyamine decomposition. Cunningham and co-workers carried out simulations of the TEMPO/S system in miniemulsion at 135 °C (not including compartmentalization effects [18]) [19], and also found that alkoxyamine decomposition is the main reaction leading to dead polymer, with similar levels of dead chains due to termination and transfer to monomer. Kruse et al. [20] concluded by use of simulations that chain transfer to monomer influenced the kinetics of the di-*tert*-butyl nitroxide/S system at 87 °C. Recent experimental and theoretical work on RAFT polymerization of 1,1-disubstituted monomers (itaconates) have indicated that chain transfer to monomer is important in these systems, causing the number-average molecular weight (M_n) to gradually deviate downwards from the theoretical M_n ($M_{n,th}$), and broadening of the MWDs [21].

This work was prompted by the recent discovery of very significant generation of new chains of low molecular weight in the dispersion NMP of S in supercritical carbon dioxide [22]. The present investigation deals with a quantitative experimental investigation into the rate of generation of new chains during NMP of S using both TEMPO at 125 °C and *N*-*tert*-butyl-*N*-(1-diethylphosphono-2,2-dimethylpropyl) nitroxide (SG1) at 110 °C (Scheme 1). Generation of new chains is confirmed using a novel technique employing a fluorescence-labelled alkoxyamine macroinitiator. It is shown that the results are quantitatively consistent with chain transfer to monomer by direct estimation of the chain transfer constant from the experimental data.

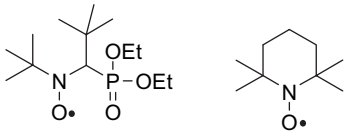

SG1

TEMPO

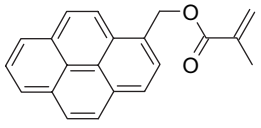

1-Pyrenylmethyl methacrylate

Scheme 1. Nitroxides and fluorescence monomer.

2. Experimental section

2.1. Materials

Styrene (S) and reagent grade toluene were purified by distillation under reduced pressure. Reagent grade 2,2′-azobis(isobutyronitrile) (AIBN; Wako) was purified by recrystallization. Benzoyl peroxide (BPO) was purified by recrystallization using chloroform/methanol. Methanol and THF were used as received. *N*-*tert*-*N*-Butyl-*N*-[1-diethylphosphono-(2,2-dimethylpropyl)] nitroxide (SG1) was synthesized according to the literature [23]. The SG1 purity was measured by ^{1}H NMR by reacting the radical with pentafluorophenylhydrazine, yielding 97% purity. TEMPO (Aldrich) and 1-pyrenylmethyl methacrylate (Polysciences Inc.) were used as received.

2.2. Polystyrene–TEMPO (PS–T) macroinitiator synthesis

A PS–T macroinitiator labelled with a small amount of the fluorescence (FL) monomer 1-pyrenylmethyl methacrylate (Scheme 1) was prepared by charging S (15.0 g, 0.144 mol), BPO (33.8 mg, 1.4×10^{-4} mol), TEMPO (27.4 mg, 1.75×10^{-4} mol) and 1-pyrenylmethyl methacrylate (14.9 mg, 4.96×10^{-5} mol) in a glass tube, followed by degassing with several N_2 cycles, sealing off under vacuum and heating at 125 °C for 4.25 h in an oil bath. The polymerization mixture was diluted with toluene and subsequently the polymer was precipitated in excess methanol, and reprecipitated several times using toluene/methanol. The obtained polymer was subsequently dissolved in toluene followed by filtration to remove unreacted FL monomer, and finally precipitated in methanol and dried in a high vacuum oven. It is crucial that the obtained PS–T is not contaminated with unreacted FL monomer, which would invalidate the subsequent FL-detector based MWD analysis. The absence of unreacted FL monomer was confirmed by GPC using FL-detection. Conversion = 46%, $M_n = 32{,}400$, and $M_w/M_n = 1.30$.

2.3. Polymerizations

The PS–T initiated polymerizations were carried out by heating S (3.14 g, 30.2 mmol) containing dissolved PS–T (0.75 g, 2.31×10^{-5} mol) in sealed glass ampoules at 125 °C in a temperature controlled oil bath. After the prescribed time the polymerization was quenched by immersing the ampoule into an ice-water bath. The polymerization mixture was dissolved/diluted in toluene, and poured into an excess of methanol to precipitate the formed polymer. Conversion was measured by gravimetry after filtration and drying. A small amount of the toluene solution was mixed with an appropriate amount of THF for GPC analysis.

The SG1-mediated polymerizations were carried out as follows: degassed toluene (2.43 g) solutions of S (2 g, 1.92×10^{-2} mol), AIBN (4.9 mg, 2.99×10^{-5} mol) and SG1 (29.4 mg, 9.93×10^{-5} mol) were heated in sealed glass ampoules at 110 °C, after which the samples were quenched

and precipitated in methanol. Conversion was measured by gravimetry as above. In these polymerizations, the GPCs correspond to the precipitated polymer.

The unusually large excess of SG1 (100% relative to the amount of alkoxyamine species formed in situ based on an AIBN initiator efficiency (f) of 0.82 [24]) was employed because these polymerizations were originally only intended for comparison with the corresponding dispersion polymerizations in supercritical carbon dioxide [22], in which case such an excess of SG1 was required.

2.4. Molecular weights

Molecular weights were measured by gel permeation chromatography (GPC) using two S/divinylbenzene gel columns (TOSOH Corporation, TSK gel GMHHR-H 7.8 mm i.d. × 30 cm) with THF as an eluent at a flow rate of 1.0 mL/min employing refractive index (RI) and fluorescence (FL) detection (TOSOH). The columns were calibrated with six linear PS samples (1.05×10^3–5.48×10^6, $M_w/M_n = 1.01$–1.15).

The $M_{n,th}$ values were calculated as follows: $M_{n,th} = (\alpha[S]_0 M_S)/[PS{-}T]_0 + M_n(PS{-}T)$ (PS–T polymerizations) and $M_{n,th} = (\alpha[S]_0 M_S)/2f[AIBN]_0$ (SG1 polymerizations), where α is S conversion, M_S and M_n (PS–T) are the molecular weights of S and PS–T macroinitiator, respectively, and $f = 0.82$ [24]. Due to the significant excess of SG1 employed, $M_{n,th}$ was calculated based on the number of radicals generated from AIBN (as opposed to the number of SG1).

2.5. Fluorescence analyses

The RI-detector response is proportional to polymer mass, whereas the FL-detector response is proportional to the concentration of FL units. The RI-detector response per polymer chain is proportional to chain length, whereas the FL-detector response per chain is proportional to the number of FL units per chain. Consequently, great care is necessary when comparing MWDs derived from RI- and FL-detection, and it is only under certain circumstances that direct comparison is possible.

The PS–T macroinitiator contained 0.063 mol% FL units (estimated from the S conversion and the FL monomer conversion from the FL-detector GPC elution trace of the polymerization mixture), which translate to approx. 20% of the PS–T chains containing one FL unit (based on $M_n = 32{,}400$), and a much lower fraction containing more than one FL unit. It is not a requirement that all chains should contain an FL unit, because the overall number of chains in the system is so high that the 20% labelled chains constitute a statistically representative sample of the full distribution. The MWD of the PS–T obtained using FL-detection was essentially identical to that using RI-detection, which indicates that the probability of any given chain containing an FL unit is proportional to its chain length (as opposed to the number of FL units incorporated being proportional to chain length, which would be the case if a sufficiently high amount of FL monomer was used).

Polymerization of S (in the absence of FL monomer) was carried out using the FL-labelled PS–T macroinitiator. Thus, if we consider a PS–T macroinitiator that contains an FL unit, the polymer formed is of the structure PS_{FL}–PS–T, where the macroinitiator PS segment contains FL, but the extended PS segment does not. Due to the different response characteristics of the RI- and FL-detector, direct comparison of the raw RI and FL GPC elution traces is of limited meaning. As an approximation, it was assumed that the chain length of PS_{FL} was proportional to the total chain length of the polymer (PS_{FL}–PS–T) (i.e. considering individual chains in the distribution). If this assumption is reasonable, then the FL response is equivalent to the RI response, i.e. the detector response per chain is proportional to the total chain length for both RI and FL, and thus the FL data can be treated in the same way as the RI data to obtain $w(\log M)$ vs. $\log M$ (the GPC distribution) and $P(M)$ vs. M (the number distribution). Careful analysis of the data revealed that this assumption was indeed reasonable, as evidenced by the $P(M)$ vs. M distributions derived from RI- and FL-detection, respectively, being close to identical in the high MW region (see Section 3).

3. Results and discussion

3.1. PS–T system

Fig. 1 shows a first-order plot of the bulk NMP of S using the fluorescence-labelled PS–T macroinitiator at 125 °C. The straight line indicates that the number of propagating radicals remains approx. constant. The PS–T macroinitiator molecular weight (MW) was deliberately chosen to be high ($M_n = 32{,}400$, $M_w/M_n = 1.30$) as this would make chain transfer to monomer easier to detect as a low MW tail. The MWDs shifted to higher MWs with increasing conversion (Fig. 2a),

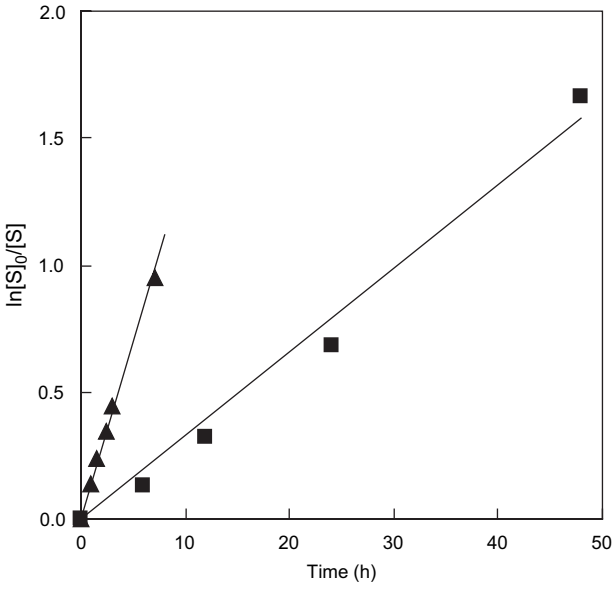

Fig. 1. First-order plots for PS–T (fluorescence-labelled; $[PS{-}T]_0 = 5.6$ mM; $M_n = 32{,}400$; $M_w/M_n = 1.30$) initiated bulk polymerization of S at 125 °C (▲) and AIBN/SG1 ($[AIBN]_0 = 5.97$ mM; $[SG1] = 19.8$ mM) initiated solution (toluene; $[S]_0 = 3.84$ M) polymerization of S at 110 °C (■).

but low MW tailing was apparent, especially as conversion increased. This tailing is much more clearly exposed by plotting the corresponding number distributions ($P(M)$; Fig. 2b) [25]. In a $P(M)$ plot, the y-values are proportional to the number of chains. The more common representation of MWDs is the so-called GPC distribution ($w(\log M)$; Fig. 2a), according to which the y-values are proportional to nM^2, where n is the number of chains and M is the molecular weight [25]. The GPC distributions (Fig. 2a) would be considered monomodal, but it is apparent that if one considers the number distributions, they are not. There is a very significant number of chains present in the low MW tail. The lowest MW in the tail ($1000 < \mathrm{MW} < 10{,}000$) remained constant despite the conversion reaching 61%, and the absolute number of chains in this region increased with conversion (the sharp peak at MW ≈ 5000). M_n increased with conversion (Fig. 3a), but gradually deviated downwards from $M_{n,th}$. The M_w/M_n values increased from 1.30 (macroinitiator) to 1.63 at 61% conversion (Fig. 3b).

Proper normalization of weight distributions (where the y-values are proportional to nM [25]) plotted vs. M, followed by transformation to $P(M)$ vs. M and subsequent integration, yields the total number of chains (N_{tot}). The weight distributions were normalized by adjusting the areas of the weight ($= w(\log M)/M$) vs. M plots to be proportional to the polymer mass in the respective system, thereby enabling further quantitative analysis [25]. The values of N_{tot} increased linearly with conversion, and the increase was as significant as 52% at 61% conversion for the PS–T experiment (Fig. 4).

The shape of $P(M)$ vs. M and N_{tot} is very sensitive to baseline errors in the low MW region of the GPC elution curve. This is illustrated in Fig. 5, which depicts the raw elution curve for the 13% conversion sample with the baseline drawn in three different ways, and the resulting $P(M)$ vs. M plots. Analysis based on baseline "b", which is clearly drawn incorrectly but yet represents a "realistic scenario", results in loss of approx. half of the low MW peak. Fig. 5 also illustrates that the low MW peak is certainly real – in order for the peak to

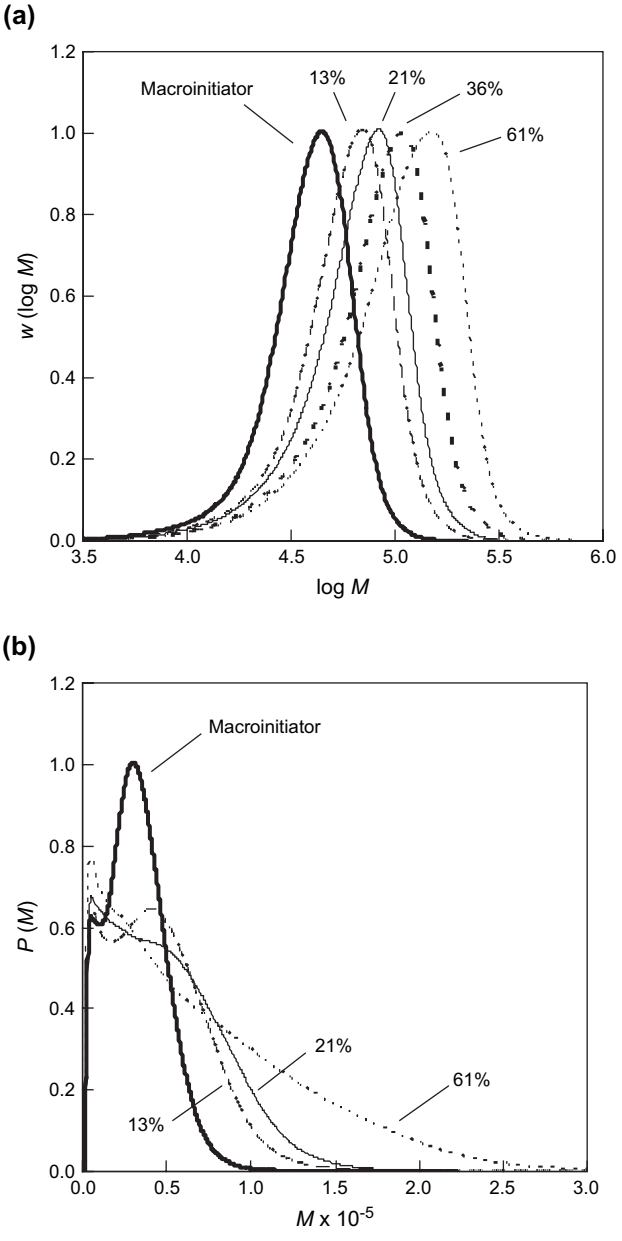

Fig. 2. PS–T initiated bulk polymerization of S at 125 °C (see Fig. 1 for details). The GPC distributions ($w(\log M)$) have been normalized to peak height (a). The number distributions $P(M)$ (36% not shown for clarity) are based on weight distributions normalized with respect to polymer mass, i.e. direct comparison is possible (b).

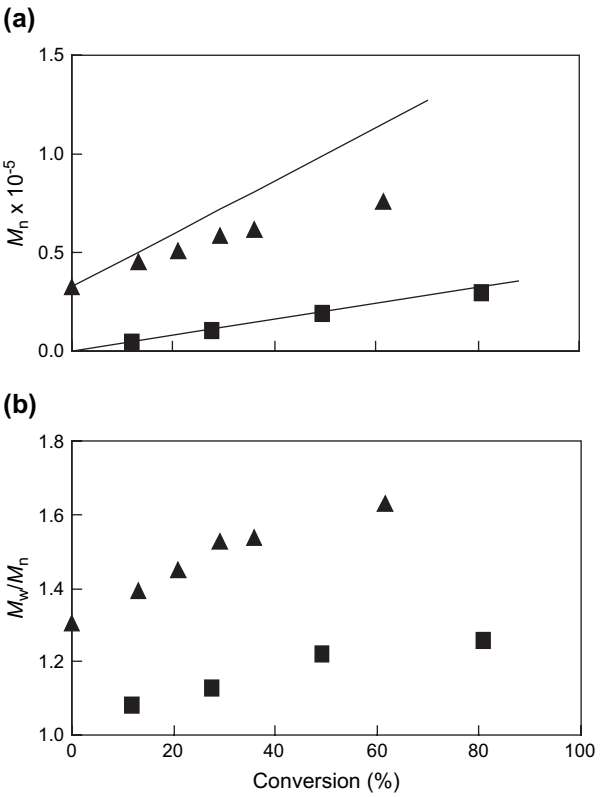

Fig. 3. M_n (a) and M_w/M_n (b) vs. conversion of PS–T (▲; 125 °C) and AIBN/SG1 (■; 110 °C) initiated polymerizations of S (see Fig. 1 for details). The lines in (a) are the theoretical M_n ($M_{n,th}$).

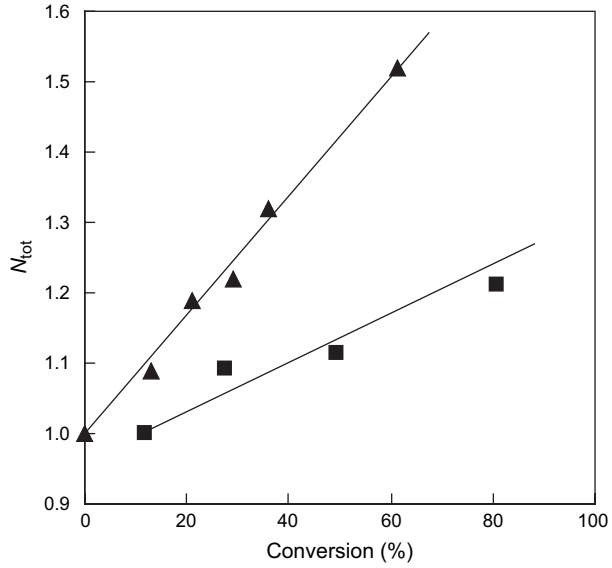

Fig. 4. Total number of chains (N_{tot}; normalized to unity at first data point) vs. conversion of PS–T (▲; 125 °C) and AIBN/SG1 (■; 110 °C) initiated polymerizations of S (see Fig. 1 for details).

disappear, the baseline has to be drawn according to "a", which is clearly incorrect. The effect of GPC sample concentration was also investigated (0.2 and 5 wt% in THF); no significant effects on the size and shape of the low MW tail were detected.

3.2. MWD analysis using fluorescence detection

The use of fluorescence detection has previously been employed in NMP to evaluate the fraction of chains containing an alkoxyamine moiety [26]. In the present study, the PS–T macroinitiator contained a small amount of the FL monomer 1-pyrenylmethyl methacrylate (Scheme 1). This approach makes it possible to distinguish between chains initiated by PS–T and chains initiated by other mechanisms, such as chain transfer to a low MW species or thermal initiation. Chains not initiated by PS–T do not contain any FL units and are thus "invisible" to the FL-detector, whereas the RI-detector "sees" all chains.

The number distributions based on RI- and FL-detection are displayed in Fig. 6. The distributions have been normalized such that the RI and FL distributions coincide for high MWs. It is evident that there is a very significant number of chains present that do not contain the original PS–T macroinitiator, as they are "invisible" to the FL-detector. The number fraction of chains without FL unit (i.e. the number fraction of chains not containing the original PS–T macroinitiator – see Section 2) decreases with increasing MW, and the contribution of such chains to the overall distribution is negligible at high MW. Moreover, the number fraction of such chains increased with conversion. These data are consistent with continuous generation of new chains throughout the polymerization, which results in the low MW tailing in the GPC MWDs (Fig. 2a) and the low MW peak in the $P(M)$ vs. M plots (Fig. 2b).

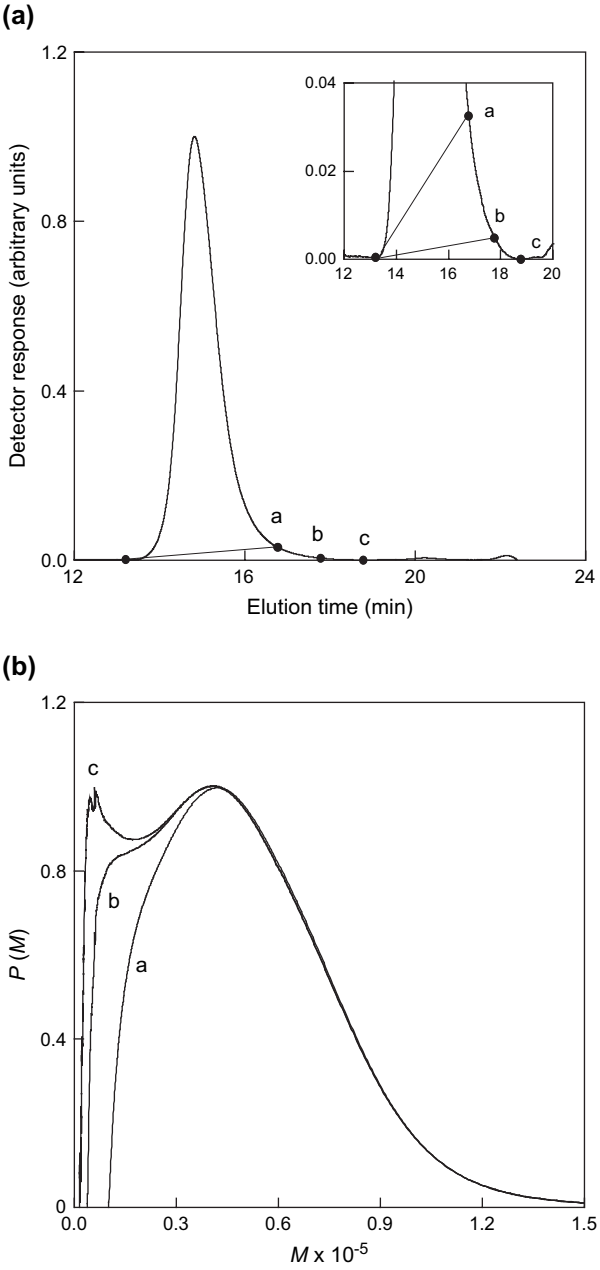

Fig. 5. RI-detector GPC elution curve of the PS–T initiated polymerization (see Fig. 1 for details) at 13% conversion (a), and the corresponding number distributions (b) obtained by drawing the baseline in (a) as straight lines as indicated.

3.3. AIBN/SG1 system

Fig. 1 shows a first-order plot of the SG1-mediated solution polymerization of S at 110 °C. The corresponding MWDs are displayed in Fig. 7. The MWDs shifted to higher MWs with increasing conversion (Fig. 7a), but a low MW tail is clearly present, especially at high conversion. This feature is as expected even more pronounced in the $P(M)$ plots (Fig. 7b). The minor differences where the lower portion of the $P(M)$ vs. M cuts the x-axis are not of any significance with regards to the polymerization kinetics. The polymers were precipitated in methanol from a toluene solution, and low MW oligomers

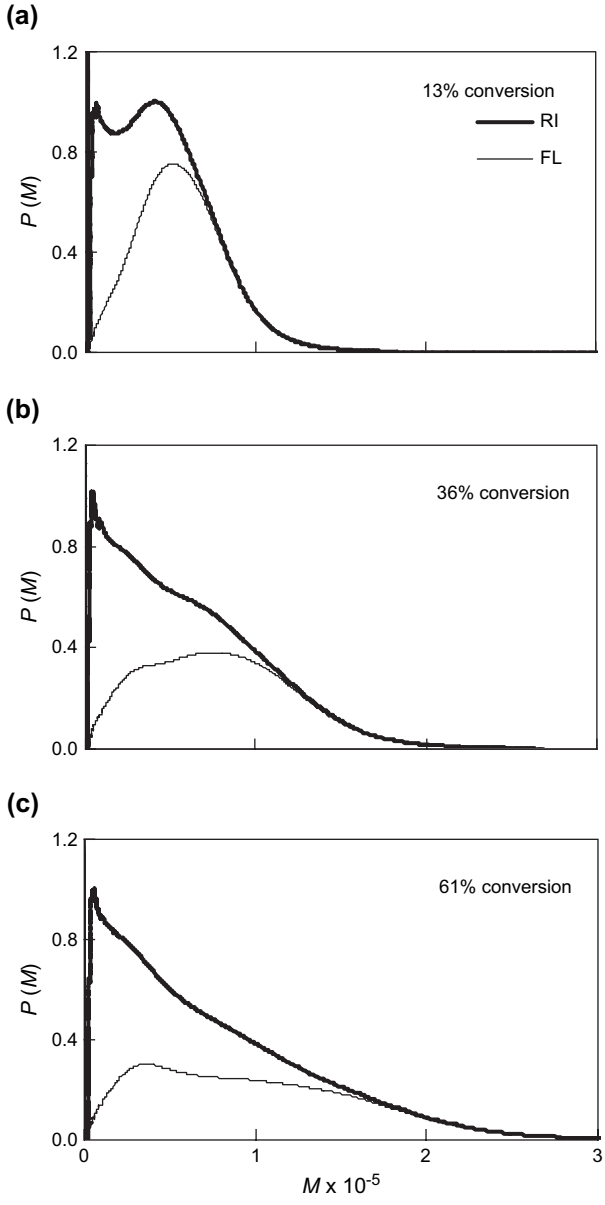

Fig. 6. Number distributions ($P(M)$) for PS–T (fluorescence-labelled) initiated bulk polymerization of S at 125 °C (see Fig. 1 for details). The thick line corresponds to all polymers in the system (RI-detector), whereas the thin line corresponds to FL-labelled polymer only, i.e. polymer containing the original FL-labelled macroinitiator. The peak heights of the RI $P(M)$ have been normalized to unity. The peak heights of the FL-derived $P(M)$ have been adjusted so that the high M regions of the RI and FL distributions coincide.

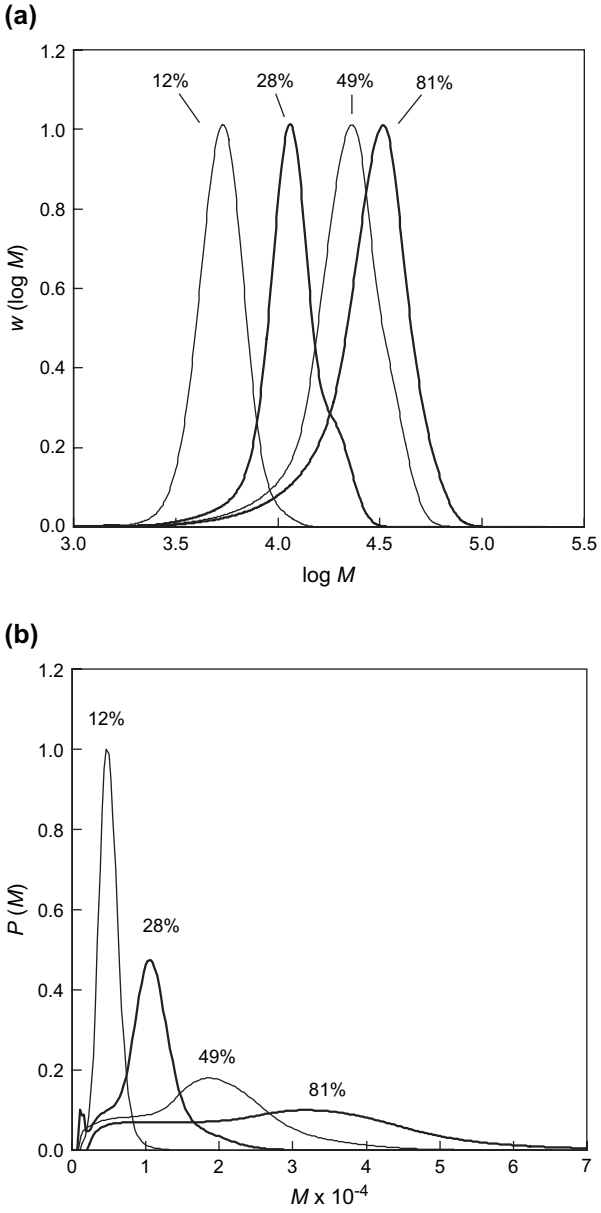

Fig. 7. AIBN/SG1 initiated solution polymerization of S at 110 °C (see Fig. 1 for details). The GPC distributions ($w(\log M)$) (a) have been normalized to peak height. The number distributions $P(M)$ (b) are based on weight distributions normalized with respect to polymer mass, i.e. direct comparison is possible.

would be lost due to non-negligible solubility in methanol. The exact pattern of loss depends on the toluene/methanol ratio, etc., and may thus differ from experiment to experiment.

The slope of the M_n vs. conversion plot (Fig. 3a) decreased with conversion, and M_w/M_n increased gradually from 1.08 at 12% to 1.26 at 81% conversion (Fig. 3b). The number of chains increased close to linearly with conversion (Fig. 4).

3.4. Chain transfer to monomer

It is proposed that the low MW peaks in both the PS–T (Figs. 2 and 6) and the AIBN/SG1 systems (Fig. 7) are mainly caused by the generation of new chains by chain transfer to monomer. Generation of monomeric radicals would occur continuously throughout the polymerization, giving rise to a population of very short chains that is present regardless of conversion as seen in Figs. 2b, 6 and 7b. These new radicals will have the same probability of undergoing growth in a controlled/living manner as radicals generated by thermal dissociation of alkoxyamine species, and consequently the distribution of new chains also shifts to higher MW with increasing conversion (Fig. 6). This continuous generation of new chains results in a gradual increase in M_w/M_n with increasing conversion (Fig. 3b), as well as $M_n < M_{n,th}$ (Fig. 3a). Similar trends in M_n and M_w/M_n have been observed experimentally for RAFT polymerization of 1,1-disubstituted monomers (itaconates),

and simulations indicated that chain transfer to monomer was a contributing factor [21]. The effect of chain transfer to monomer is stronger in the PS–T system (125 °C) than in the AIBN/SG1 system (110 °C) because: (i) $M_{n,th}$(PS–T) > $M_{n,th}$(AIBN/SG1). Higher $M_{n,th}$ means fewer initial chains, and thus a greater number fraction of new chains due to chain transfer to monomer. Moreover, the low MW tail becomes more apparent in the MWD when the MW of the main peak is higher; (ii) the chain transfer constant, $C_{tr,M}$ (=$k_{tr,M}/k_p$, where $k_{tr,M}$ and k_p are the rate coefficients for chain transfer to monomer and propagation, respectively), increases with temperature; $E_{tr,M} = 56.7$ kJ mol^{-1} (see below), $E_p = 32.5$ kJ mol^{-1} [27].

Based on the assumption that $C_{tr,M}$ remains constant throughout the polymerization [28], the concentration of new chains generated by chain transfer to monomer ([chain$_{tr,M}$]) is proportional to the fractional monomer conversion (α) according to:

$$[\text{chain}_{tr,M}] = \alpha[M]_0 C_{tr,M} \quad (1)$$

where $[M]_0$ is the initial monomer concentration. Eq. (1) predicts that the number of new chains (and N_{tot}) should increase linearly with conversion if chain transfer to monomer is the main source of new radicals, consistent with the experimental data (Fig. 4).

In an NMP system where the only source of new chains is chain transfer to monomer, the following expression describes the number fraction of chains derived from chain transfer to monomer ($X_{tr,M}$):

$$X_{tr,M} = \frac{\alpha[M]_0 C_{tr,M}}{\alpha[M]_0 C_{tr,M} + [PT]_0} \quad (2)$$

where $[PT]_0$ denotes the initial alkoxyamine concentration. Rearrangement yields:

$$\frac{1}{X_{tr,M}} = 1 + \frac{[PT]_0}{[M]_0 C_{tr,M}} \frac{1}{\alpha} \quad (3)$$

According to Eq. (3), a plot of $1/X_{tr,M}$ vs. $1/\alpha$ yields a straight line with slope $[PT]_0/([M]_0 C_{tr,M})$. In a real S NMP system, thermal initiation and termination (mainly by combination) also occur, and both of these events alter the total number of chains. Before plotting the experimental data according to Eq. (3), the data were corrected for the contribution of thermal initiation. The total number of chains (N_{tot}) is expressed as:

$$N_{tot} = N_0 + N_{tr,M} + N_{thermal} \quad (4)$$

where N_0 is the initial number of chains, and $N_{tr,M}$ and $N_{thermal}$ are the numbers of chains generated by chain transfer to monomer and thermal initiation, respectively. $X_{tr,M}$ (as defined by Eq. (2)) is thus given by:

$$X_{tr,M} = (N_{tot} - N_0 - N_{thermal})/(N_{tot} - N_{thermal}) \quad (5)$$

The value of N_{tot} was obtained by integration of the properly normalized number distributions (i.e. the number distributions corresponding to the properly normalized weight vs. M distributions, see Section 3.1). In the PS–T initiated polymerization, the increase in the number of chains at the first data point can be evaluated relative to the point at $t = 0$ (i.e. the unreacted macroinitiator). In the AIBN/SG1 system, there is no polymer at $t = 0$, and therefore zero conversion is redefined to correspond to the first data point at $\alpha = 12.1\%$, and the conversions at all subsequent data points are adjusted accordingly (e.g., $\alpha = 27.7\%$ becomes $(27.7 - 12.1)/(100 - 12.1) = 17.7\%$). The value of $[M]_0$ in Eq. (3) thus corresponds to $\alpha = 12.1\%$ ($[M]_0 = 3.38$ M). $[PT]_0$ in Eq. (3) was obtained from $2f[AIBN]_0$ ($f = 0.82$ [24]), and by assuming that the rate of increase in number of chains relative to conversion (linear, as shown in Fig. 4) was the same between $\alpha = 0$ and 12.1% as for $\alpha > 12.1\%$, resulting in $[PT]_0 = 1.84$ mM. $N_{thermal}$ was computed from $R_{i,th} = k_{i,th}[M]^3$ ($k_{i,th} = 4.26 \times 10^{-11}$ and 1.67×10^{-10} M^{-2} s^{-1} at 110 and 125 °C, respectively, [29]) by numerical integration of $k_{i,th}[M]^3$ with respect to time using the experimentally obtained time-dependences of [M] (Fig. 1). The contributions of chains from thermal initiation (($N_{thermal}/N_{tot}$) × 100%) were 6.0% (PS–T; 61% conv.) and 1.5% (AIBN/SG1; 81% conv.). The number fraction of chains that undergoes termination in a CLRP system is in general low (in particular in the presence of a vast excess of nitroxide as in the AIBN/SG1 system), and no attempt was made to correct for the effect of this on N_{tot}. It cannot be excluded that a small fraction of new chains may be derived from chain transfer to impurities or by other unknown mechanisms; however, this fraction is deemed to be insignificant in comparison with the number of chains originating from chain transfer to monomer and thermal initiation.

Fig. 8 shows plots of $1/X_{tr,M}$ vs. $1/\alpha$ for the systems PS–T and AIBN/SG1. Straight lines according to Eq. (3) were fitted to both data sets using least-squares fitting, resulting in $C_{tr,M} = 4.83 \times 10^{-4}$ and 6.89×10^{-4} for the PS–T system at 125 °C and the AIBN/SG1 system at 110 °C, respectively, which in turn gives $k_{tr,M} = 1.12$ (125 °C) and 1.09 M^{-1}s^{-1} (110 °C) based on the IUPAC-recommended values of k_p for S [27]. The entire data set of chain transfer to monomer constants for S in the Polymer Handbook [30] was recalculated to $k_{tr,M}$ based on the IUPAC-recommended k_p Arrhenius parameters for S [27]. The resulting $k_{tr,M}$ values are displayed in Fig. 9 in the form of an Arrhenius plot covering the temperature range 0–132 °C. A best fit results in $E_{tr,M} = 56.7$ kJ mol^{-1} and $A_{tr,M} = 2.0 \times 10^7$ M^{-1} s^{-1}. The $k_{tr,M}$ values obtained in the present study by use of Eq. (3) have been included in Fig. 9 (filled circles), illustrating good agreement with the Polymer Handbook data.

3.5. Other sources of small radicals

It has been shown that significant generation of new chains occurs in the present systems, and it is proposed that this is mainly caused by chain transfer to monomer. However, there are other conceivable sources of small radicals, the most obvious being thermal (“spontaneous”) initiation of S [29]. Based on the rate of generation of thermal radicals being equal

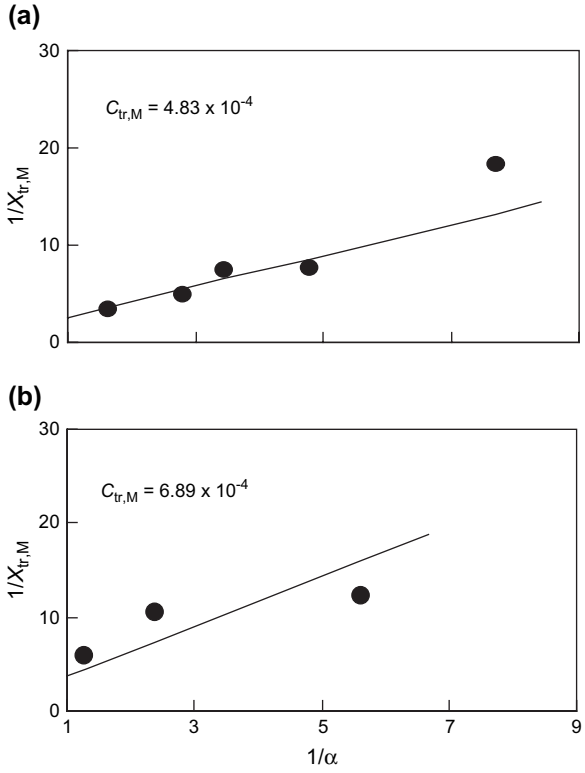

Fig. 8. Plots of $1/X_{tr,M}$ vs. $1/\alpha$ according to Eq. (3) for PS–T (a; 125 °C) and AIBN/SG1 (b; 110 °C) initiated polymerizations of S (see Fig. 1 for details). The lines are best fits according to Eq. (3), resulting in $C_{tr,M}$ as indicated.

to $k_{i,th}[M]^3$ and the dependence of [M] on time in Fig. 1 for the PS–T initiated polymerization, $k_{i,th} = 1.62 \times 10^{-9}$ $M^{-2}s^{-1}$ is required to account for all new chains generated at 61% conversion. This is approx. one order of magnitude greater than the literature value at 125 °C ($k_{i,th} = 1.67 \times 10^{-10}$ M^{-2} s^{-1}) [29].

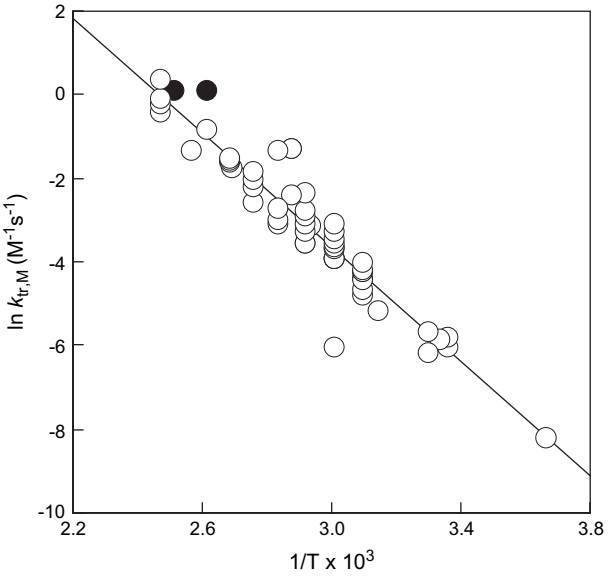

Fig. 9. Arrhenius plot of the rate coefficient for chain transfer to monomer in S radical polymerization ($k_{tr,M}$) as obtained from the chain transfer constants ($C_{tr,M}$) in the Polymer Handbook and the IUPAC-recommended k_p Arrhenius parameters for styrene [27]. The filled circles correspond to the $C_{tr,M}$ values obtained by fitting according to Eq. (3) (Fig. 8).

The nitroxide SG1 decomposes at high temperature with a half-life of 15 h at 120 °C [12]. This decomposition has been reported to be accompanied by radical generation and subsequent initiation [24]. A large excess of SG1 (100% relative to the amount of alkoxyamine species formed in situ based on $f_{AIBN} = 0.82$) was employed in the present study, and assuming that SG1 decomposition only occurs when SG1 is in the dissociated state, it is plausible the large excess of SG1 employed would lead to an increased rate of generation of new chains via this mechanism. However, the use of only 10% excess SG1 resulted in very similar low MW broadening, revealing that this mode of generation of new chains is not important within the current context [22].

4. Conclusions

Very significant generation of new chains throughout the polymerization has been detected during NMP of S using both TEMPO at 125 °C and SG1 at 110 °C. These new chains, which are kinetically indistinguishable from chains originally generated by thermal dissociation of polymeric alkoxyamines, mainly grow in a controlled/living manner, and thus their distribution shifts to higher MW with increasing conversion, although a significant number fraction remains at very low MWs due to the continuous generation of new chains. Use of a fluorescence-labelled PS–T macroinitiator enabled separate detection of the total chain distribution and the distribution of chains containing the original macroinitiator, directly confirming the presence of chains not containing the macroinitiator.

It is proposed that the main origin of these new chains is chain transfer to S. The total number of chains increased linearly with conversion, consistent with chain transfer to S. Analysis of the total number of chains (based on the assumption that all new chains were caused by chain transfer to S, and correcting for thermal initiation) yielded chain transfer constants in good agreement with the Polymer Handbook [30]. These results, in addition to being of importance with regards to the fundamentals of CLRP, have implications concerning investigations of livingness in S-based NMP systems by chain-extension experiments (which are based on negligible generation of new chains during chain extension).

Acknowledgements

This work was partially supported by the Support Program for Start-ups from Universities (no. 1509), from the Japan Science and Technology Agency (JST), a Grant-in-Aid for Scientific Research (Grant 17750109) from the Japan Society for the Promotion of Science (JSPS), a Kobe University Takuetsu-shita Research Project Grant, and an Embark Postgraduate Scholarship from the Irish Research Council for Science, Engineering and Technology (IRCSET).

References

[1] Matyjaszewski K. Advances in controlled/living radical polymerization. Washington, DC: American Chemical Society; 2003.
[2] Goto A, Fukuda T. Prog Polym Sci 2004;29:329–85.
[3] Hawker CJ, Bosman AW, Harth E. Chem Rev 2001;101:3661–88.
[4] Matyjaszewski K, Xia J. Chem Rev 2001;101:2921–90.
[5] Moad G, Rizzardo E, Thang SH. Aust J Chem 2005;58:379–410.
[6] Li I, Howell BA, Matyjaszewski K, Shigemoto T, Smith PB, Priddy DB. Macromolecules 1995;28:6692–3.
[7] Goto A, Kwak Y, Yoshikawa C, Tsujii Y, Sugiura Y, Fukuda T. Macromolecules 2002;35:3520–5.
[8] Ananchenko GS, Fischer H. J Polym Sci Part A Polym Chem 2001;39:3604–21.
[9] Ohno K, Tsujii Y, Fukuda T. Macromolecules 1997;30:2503–6.
[10] He J, Yang Y. Macromolecules 2000;33:2286–9.
[11] Gridnev AA. Macromolecules 1997;30:7651–4.
[12] Marque S, LeMercier C, Tordo P, Fischer H. Macromolecules 2000;33:4403–10.
[13] Nilsen A, Braslau R. J Polym Sci Part A Polym Chem 2005;44:697–717.
[14] Fischer H. J Polym Sci Part A Polym Chem 1999;37:1885–901.
[15] Pryor WA, Coco JH. Macromolecules 1970;3:500–8.
[16] Moad G, Solomon DH. The chemistry of radical polymerization. 2nd ed. Oxford: Elsevier; 2006. p. 317.
[17] Greszta D, Matyjaszewski K. Macromolecules 1996;29:7661–70.
[18] Zetterlund PB, Okubo M. Macromolecules, in press.
[19] Ma JW, Cunningham MF, McAuley KB, Keoshkerian B, Georges MK. Chem Eng Sci 2003;58:1163–76.
[20] Kruse TM, Souleimonova R, Cho A, Gray MK, Torkelson JM, Broadbelt LJ. Macromolecules 2003;36:7812–23.
[21] Szablan Z, Toy AA, Terrenoire A, Davis TP, Stenzel MH, Mueller AHE, et al. J Polym Sci Part A Polym Chem 2006;44:3692–710.
[22] McHale R, Aldabbagh F, Zetterlund PB, Minami H, Okubo M. Macromolecules 2006;39:6853–60.
[23] Cuervo-Rodriguez R, Bordege V, Fernandez-Monreal MC, Fernandez-Garcia M, Madruga EL. J Polym Sci Part A Polym Chem 2004;42:4169–76.
[24] Lacroix-Desmazes P, Lutz J-F, Chauvin F. Macromolecules 2001;34:8866–71.
[25] Gilbert RG. Trends Polym Sci 1995;3:222–6.
[26] Scott ME, Parent JS, Hennigar SL, Whitney RA, Cunningham MF. Macromolecules 2002;35:7628–33.
[27] Buback M, Gilbert RG, Hutchinson RA, Klumperman B, Kuchta FD, Manders BG, et al. Macromol Chem Phys 1995;196:3267–80.
[28] Casey BS, Mills MF, Sangster DF, Gilbert RG, Napper DH. Macromolecules 1992;25:7063–5.
[29] Hui AW, Hamielec AE. J Appl Polym Sci 1972;16:749–69.
[30] Ueda A, Nagai S. Transfer constants to monomers, polymers, catalysts and initiators, solvents and additives, and sulfur compounds in free radical polymerization. In: Brandrup J, Immergut EH, Grulke EA, editors. Polymer handbook. 4th ed. New York: John Wiley & Sons; 1999. p. II/102.